

Surface Tension of a Topological Phase

Saikat Mondal^{1,*} and Adhip Agarwala^{1,†}

¹*Department of Physics, Indian Institute of Technology Kanpur, Kalyanpur, UP 208016, India*

Metastable phases, in general, are unstable to nucleating droplets of the order defining the global free energy minima. However, whether such a droplet grows or shrinks relies on a competition between the surface tension and bulk energy density. We study the role of coupling a topological fermionic field to a scalar field undergoing such nucleation processes. We find that existence of non-trivial fermionic boundary modes on the nucleating droplets leads to substantial quantum corrections to the surface tension thereby modifying the size of the critical nucleus beyond which unrestricted droplet growth happens. To illustrate the phenomena we devise a minimal model of fermions in a Chern insulating system coupled to a classical Ising field in two spatial dimensions. Using a combination of analytic and numerical methods we conclusively show that topological phases can lead to characteristic quantum surface tension. Apart from material systems, our work has implications on the interplay of physics of statistical classical fields and quantum topological order.

Introduction: The physics of nucleation, where a droplet of order defining the global energy minima grows or shrinks within a metastable phase is one of the defining tenets within the study of phases and phase transitions [1–3]. These ideas govern a wide range of phenomena spanning condensed matter [4–6], nuclear physics [7–13] and high-energy field theories [14–20]. The conditions on growth and decay of any such nuclei, however, are governed by a competition between the surface tension and bulk free-energy density [21–23]. Microscopic models have been devised to make quantitative predictions and study the physical processes such as crystal growth, domain formation and role of thermal excitations and impurity effects [6, 24–28]. With advances in computational methods and new experimental platforms, many of these ideas have been investigated ranging from material to colloidal systems [29–32]. While dominantly studied in classical systems, the role of surface tension and nucleation physics vis-a-vis quantum fluctuations have been little explored [33].

In this work we pose – can a topological fermionic field, when coupled to a scalar field, modify the physics of nucleation? Topological phases of matter, due to non-trivial topological terms in the fermionic field theory, retain edge-modes even when the bulk is gapped. These have ushered in a new paradigm in search of exotic phases of quantum matter with potential technological applications [34–36]. Vigorous experimental and theoretical search has now lead to a gallery of such phases and has subsumed systems such as integer quantum Hall as their early examples [37, 38]. While studied as a stand alone quantum phenomena - their interplay with the nucleation process of classical statistical fields haven't been explored. Here, we conclusively show that coupling such a fermionic system to an Ising field can significantly modify the latter's nucleation physics. While our investigation here is theoretical, such systems of coupled fermionic degrees of freedom with Landau like scalar order parameters have been of immense interest given their direct applicability to a range of material platforms including

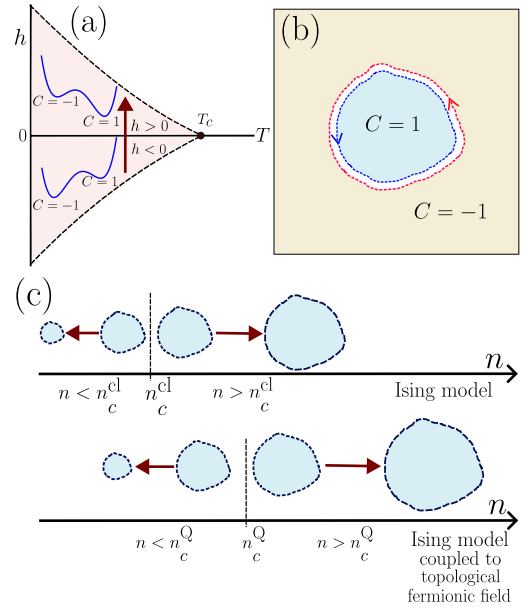


FIG. 1. Growth and shrinking of cluster: (a) Schematic diagram of free-energy density (denoted by blue curves) for two-dimensional classical Ising model in external magnetic field $h > 0$ and $h < 0$, at temperature $T < T_c$, where T_c is critical temperature. C denotes Chern number for the situation when Ising field is coupled to topological fermionic field. Arrow indicates the sudden quench from $h < 0$ to $h > 0$ when $T < T_c$. (b) Schematic diagram of a droplet having Chern number $C = 1$ within metastable region having $C = -1$. (c) Growth and shrinking of droplet of size n , where n_c^{cl} and n_c^Q are critical cluster-sizes for nucleation in classical Ising model and in the situation when Ising field is coupled to topological fermionic field respectively. Here, $n_c^Q > n_c^{cl}$.

those of anomalous quantum Hall systems, spintronics and physics of correlated topological phenomena [39–49].

In this study we limit to a scalar Ising field in two dimensions which undergoes the standard order-disorder transitions in the magnetic field (h) and temperature (T) plane (see Fig. 1(a)) where the second order thermal phase transition happens at $T = T_c$ [50]. We couple

a two dimensional fermionic Dirac theory to the Ising field in such a way that the order parameter of the scalar field acts like the effective mass for the Dirac fermions. Thus the free-energy minima for $h > 0$ and $h < 0$ (for $T < T_c$) regime also correspond to topological insulating phases (for fermions) albeit with different Chern numbers ($C = \pm 1$). We perform a gedanken experiment where a quench is done from $h < 0$ to $h > 0$ regime such that system is in a metastable phase of $C = -1$ with spins down polarized while the global free-energy minima is for the $C = +1$ phase with spins up polarized. We now investigate the stability of a bubble of $C = +1$ region created within this metastable phase (see Fig. 1(b)). In absence of any fermionic field it is known that a bubble only beyond a critical size n_c^{cl} would grow transforming the phase to the one defining the global free energy minima. This essentially is governed by the fact that the gain in the bulk free energy is higher than the surface tension costs involved in the expansion process. Interestingly the metastable phase is stable to droplets of nuclei size $n < n_c^{\text{cl}}$ where any such droplet shrinks with time. Presence of a topological fermionic field when coupled to a scalar field leads to quantum corrections to the surface tension. This is essentially the result of chiral edge or surface modes on the droplet boundary due to the topological character of fermions (see Fig. 1(b)). This quantum surface tension leads to an enhancement of the critical nuclei size to n_c^{Q} such that n_c^{Q} is always greater than n_c^{cl} (see Fig. 1(c)). In fact as we will show such enhancement can be tuned by changing the microscopic parameters of theory, easily achieving $n_c^{\text{Q}}/n_c^{\text{cl}} \sim 2 - 3$ within experimentally relevant scales.

Model: We consider Bernevig-Hughes-Zhang (BHZ) model [51] of spinless fermions coupled to two-dimensional ferromagnetic classical Ising model on a square lattice, such that the Hamiltonian is

$$H = -\kappa \sum_i s_i \Psi_i^\dagger \sigma_z \Psi_i - \sum_{\langle ij \rangle} (\Psi_i^\dagger \eta_{ij} \Psi_j + \text{h.c.}) - J \sum_{\langle ij \rangle} s_i s_j - h \sum_i s_i, \quad (1)$$

where the spin variable for i -th unit cell can assume $s_i = \pm 1$ and $J > 0$. Each unit cell contains A and B sites having staggered masses $\pm \kappa s_i$. The hopping strengths between nearest neighboring unit cells along x -axis and y -axis are $\eta_{ij} = \frac{1}{2}(\sigma_z + i\sigma_x)$ and $\eta_{ij} = \frac{1}{2}(\sigma_z + i\sigma_y)$ respectively where $\sigma_x, \sigma_y, \sigma_z$ are Pauli matrices and $\Psi_i = (c_{iA} \ c_{iB})^T$ with $c_{iA} (c_{iB})$ being annihilation operator of fermion at site $A (B)$ of i -th unit cell. κ is coupling parameter between the fermions and the Ising spins. We keep fermionic filling fixed at half. When $\kappa = 1$, an up polarized state with magnetization $m = \frac{1}{L^2} \sum_i \langle s_i \rangle = +1$ corresponds to a fermionic Chern insulator with $C = +1$ and a down polarized state ($m = -1$) leads to a fermionic Chern insulator with $C = -1$. Moreover at $T = 0$, κ it-

self can be tuned such that when $0 < |\kappa| < 2$ we have a topological phase with $C = \pm 1$ and a trivial phase with $C = 0$ when $|\kappa| > 2$ [51–53]. We will consider periodic boundary conditions in the square lattice throughout our work.

Let us now consider the system being subjected to a sudden quench of external field from $h < 0$ to $h > 0$ (keeping $|h|$ fixed) at a fixed temperature $T < T_c$. In other words, the system is suddenly quenched from the ferromagnetic phase with negative magnetization to another ferromagnetic phase with positive magnetization. As $h < 0$ before the quench, $s_i = -1$ for all unit cells. As quench is performed suddenly, most of the unit cells remain in down-spin ($s_i = -1$) metastable state while only few unit cells are in up-spin state ($s_i = 1$) immediately after the quench, thus leading to the formation of cluster of up-spins within metastable state of down-spins. Depending on initial (i.e. immediately after quench) size n of cluster with up-spins, the cluster either grows or shrinks, as we discuss below.

Quantum correction to surface tension: When $\kappa = 0$, the fermions and spins are decoupled and therefore the physics of nucleation under the quench protocol is determined by just the classical Ising fields. In this situation, the change of free-energy in the formation of a circular cluster of size n is

$$\Delta F_{\text{classical}} = -2|h|n + 2\sqrt{\pi n} \sigma_{\text{cl}}, \quad (2)$$

where $\sigma_{\text{cl}} > 0$ is the surface tension which depends on J and temperature T [2, 26]. When $\kappa = 0$, change of free energy $\Delta F_{\text{classical}}$ is maximum for critical cluster-size

$$n_c^{\text{cl}} = \frac{\pi \sigma_{\text{cl}}^2}{4|h|^2}. \quad (3)$$

Thus, to reduce the free energy, the cluster grows with time when $n > n_c^{\text{cl}}$ and it shrinks when $n < n_c^{\text{cl}}$. This is essentially determined by a competition of the surface tension with the bulk energy-density and a system with a higher surface tension σ_{cl} would pertain to a larger n_c^{cl} .

When $\kappa \neq 0$, the Ising field and the fermionic system are coupled thus changing the total free-energy of the system. This in turn can influence the physics of nucleation. Under the same quench protocol, the total change of free-energy ΔF is

$$\Delta F = \Delta F_{\text{classical}} + \Delta E. \quad (4)$$

where ΔE is the contribution from the fermionic field which can again have both surface and bulk contributions. The bulk contribution from the fermionic field is close to zero since in the nucleating droplet there is a flip of the effective mass term $M_{\text{eff}} \equiv \kappa m$ under which the ground state energy of the fermionic system at half-filling doesn't change. The surface contributions to ΔE are however non-trivial given the fermionic phases are

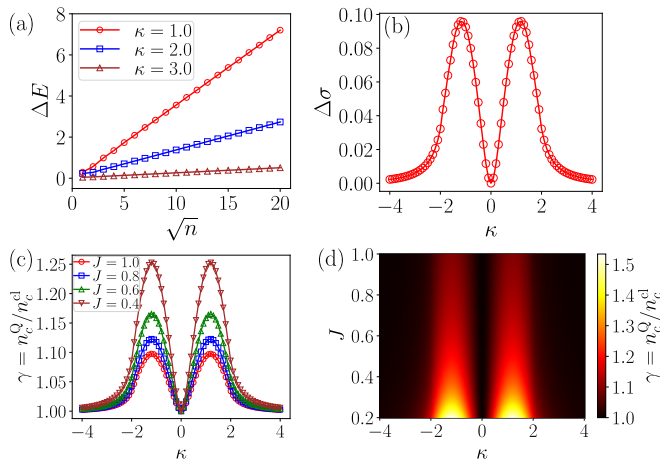


FIG. 2. **Surface tension and critical cluster-size:** (a) Change of ground-state energy ΔE (see text) due to quantum fluctuation ($\kappa \neq 0$) in sudden quench from $h < 0$ to $h > 0$ as a function of \sqrt{n} where n is droplet-size with up-spins. (b) Quantum correction to surface tension $\Delta\sigma$ as a function of κ . Here, $\Delta\sigma$ is obtained from the slope (see Eq. (5)) of linearly fitted plot of ΔE with \sqrt{n} in (a). (c) $\gamma = n_c^Q/n_c^{\text{cl}}$ (as defined in Eq. (7)) as a function of κ for various values of J at temperature $T = 0$, where n_c^{cl} is the critical cluster-size for classical Ising model ($\kappa = 0$). (d) γ as a function of κ and J at temperature $T = 0$. For all the plots, total number of unit cells in square lattice is $L^2 = 1024$.

topologically distinct which leads to chiral edge states on the boundary of the droplet.

To estimate ΔE we compare the ground state energies ($h = 0, T = 0$) between configurations (i) where a square region of size L^2 has all $s_i = -1$ and another (ii) where an internal region of size l^2 (where $l = \sqrt{n}$) has $s_i = +1$ while the rest of $s_i = -1$. Variation of ΔE shows a characteristic \sqrt{n} dependence for a finite κ (see Fig. 2(a)), thus leading to a quantum contribution to surface tension ($\Delta\sigma$) which can be estimated from the slope as

$$\Delta E = 4(\Delta\sigma)\sqrt{n}, \quad (5)$$

where $4\sqrt{n}$ is the perimeter of the internal region. Furthermore $\Delta\sigma$ has an interesting dependence on κ which we discuss next.

As shown in Fig. 2(b), $\Delta\sigma \rightarrow 0$ when $\kappa \rightarrow 0$ reflecting the decoupled limit. However $\Delta\sigma$ is significantly large when $0 < |\kappa| < 2$ and falls when $|\kappa| > 2$ (see supplemental material SM [54] for details). This again is directly related to the fact that the fermionic problem is topological when $|M_{\text{eff}}| < 2$ and trivial for $|M_{\text{eff}}| > 2$. Thus the $\Delta\sigma$ is primarily determined by the edge state energy per unit length ($\Delta\epsilon_{\text{edge}}$) of the boundary of a nucleating droplet. An analytical estimate of $\Delta\epsilon_{\text{edge}}$ and its comparison with $\Delta\sigma$ are shown in SM [54].

When $\kappa \neq 0$, the total change of free energy ΔF is

maximum for the critical circular cluster-size

$$n_c^Q = \frac{\pi(\sigma_{\text{cl}} + \Delta\sigma)^2}{4|h|^2}. \quad (6)$$

Thus the enhancement of critical nuclei of the classical Ising field, due to its coupling to the fermionic field ($\kappa \neq 0$) can be quantified by defining

$$\gamma = \frac{n_c^Q}{n_c^{\text{cl}}} = \left(1 + \frac{\Delta\sigma}{\sigma_{\text{cl}}}\right)^2. \quad (7)$$

Interestingly, γ behaves non-monotonically with κ , mirroring the behavior of $\Delta\sigma$. The interplay of Ising spin-exchange scale J and the edge-mode contribution to $\Delta\sigma$ allows for further tunability of γ . At $T = 0$, the surface tension in classical Ising model is $\sigma_{\text{cl}} = 2J$ which implies an increase in γ with decreasing J (see Fig. 2(c,d)). For $J \sim 0.2$ and $\kappa \sim 1$, one can tune $\gamma \sim 1.5$ which is upto 50% rise in the size of critical nuclei. To study if this physics remains stable under thermal fluctuations, we now analyze the system at finite temperatures.

Growth and shrinking of clusters at finite temperature: At finite T (compared to J scales), thermal fluctuation reduces the stiffness of the domain wall thereby reducing σ_{cl} from its zero temperature value ($2J$) [26]. It is useful to note we work with $T < T_c$ where the classical transition temperature $T_c \approx 2.269J$ [50] (where Boltzmann constant is set to unity). Assuming that the fermionic energy scales, given a finite large Fermi energy, do not significantly depend on temperatures - we expect that γ increases with T ($T < T_c$).

For numerical computation of n_c^{cl} and n_c^Q at finite $\beta = 1/T$, we resort to Monte Carlo (MC) simulation [55] (see SM [54] for details). Here we work within the assumption that electronic time-scales are much faster than the spin time-scales such that electronic equilibration happens immediately leading to just internal energy corrections to the spin configurations within the Metropolis algorithm [55]. We start from an initial configuration with $n = l^2$ sites in up-spin configuration while the rest of the spins are in the down configuration. We then investigate the quantity

$$\nu(n) = \frac{P_+(n) - P_-(n)}{P_+(n) + P_-(n)} \quad (8)$$

where $P_+(n)$ and $P_-(n)$ count the number of MC steps in which the size n of a cluster increases to $(n + 1)$ and decreases to $(n - 1)$ respectively [6]. The critical cluster-sizes n_c^{cl} and n_c^Q are then obtained from when ν crosses 0 in MC simulations for $\kappa = 0$ and $0 < |\kappa| < 2$ respectively, where $n_c^Q > n_c^{\text{cl}}$ (see Fig. 3(a)). It is important to note that temperature T considered in MC simulation is much smaller than the fermionic energy-scales, thus the effect of thermal fluctuation on quantum surface tension can be ignored.

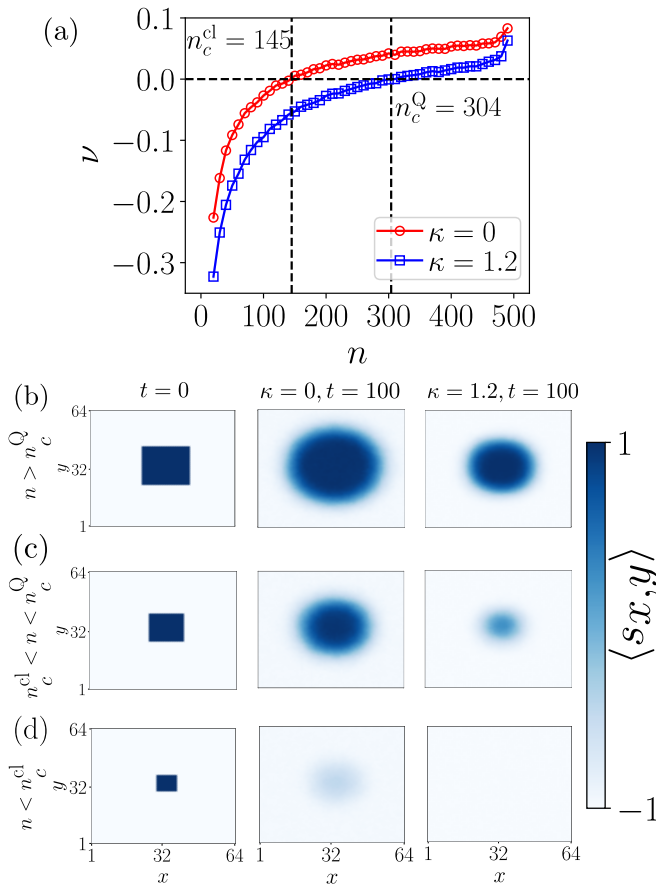


FIG. 3. **Critical cluster-size and average local magnetization:** (a) ν (as defined in Eq. (8)) as a function of cluster size n . Critical cluster-sizes $n_c^{\text{cl}} = 145$ and $n_c^{\text{Q}} = 304$ for $\kappa = 0$ and $\kappa = 1.2$ are obtained from $\nu = 0$. (b, c, d) Average local magnetization $\langle s_{x,y} \rangle$ for the unit cell with coordinate (x, y) for a cluster of up-spins having initial size (b) $n = 441$ ($n > n_c^{\text{Q}}$), (c) $n = 225$ ($n_c^{\text{cl}} < n < n_c^{\text{Q}}$), (d) $n = 81$ ($n < n_c^{\text{cl}}$) at times $t = 0$ and $t = 100$ (in the units of Monte Carlo steps per site) when $\kappa = 0$ and $\kappa = 1.2$. In all the plots, the parameters chosen are: $J = 0.2$, $T = 1/\beta = 0.33$ (where $T_c \approx 0.45$), $h = 0.02$. The number of unit cells in square lattice is $L^2 = 4096$ and number of simulations considered is 1000.

Now, to observe the growth (shrinkage) of clusters with time t , we calculate average local magnetization $\langle s_{x,y} \rangle$ for any unit cell at position $\mathbf{r} = (x, y)$ as a function of t (see SM [54] for details). The behavior of $\langle s_{x,y} \rangle$ for different values of κ and t is shown in Fig. 3(b-d). Our study reveals that when initial size of cluster (having up-spins) $n > n_c^{\text{Q}}$, the cluster grows in size with time in both classical Ising model ($\kappa = 0$) and topological ($0 < |\kappa| < 2$) situations, while when $n < n_c^{\text{cl}}$, the size of the cluster shrinks for both $\kappa = 0$ and $0 < |\kappa| < 2$. However, when $n_c^{\text{cl}} < n < n_c^{\text{Q}}$, although the cluster grows in size for $\kappa = 0$, it shrinks for $0 < |\kappa| < 2$ (see Fig. 3(b-d)), thus establishing the role of topological surface tension in altering growth (shrinkage) of clusters.

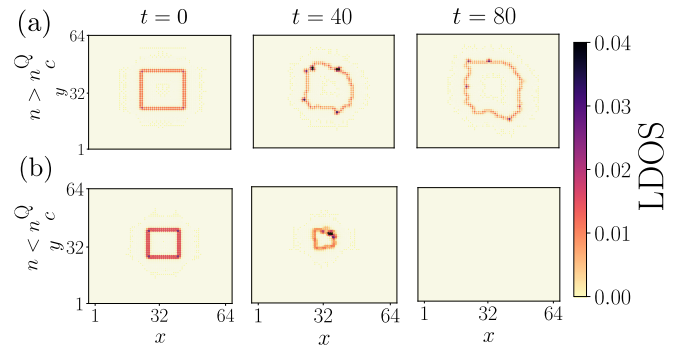


FIG. 4. **Edge-state evolution:** Local density of states (LDOS) of edge-modes for initial cluster-sizes (a) $n = 441$ ($n > n_c^{\text{Q}}$), (b) $n = 225$ ($n < n_c^{\text{Q}}$) at times $t = 0, 40, 80$ (in the units of Monte Carlo steps per site), where $n_c^{\text{Q}} = 304$. The parameters chosen here are: $J = 0.2$, $T = 1/\beta = 0.33$ (where $T_c \approx 0.45$), $h = 0.02$, $\kappa = 1.2$. The number of unit cells in square lattice is $L^2 = 4096$.

Edge-state evolution: In order to observe the edge-states in the nucleating droplet, we take a typical spin configuration in the MC evolution and solve the fermionic problem to obtain the local density of states (LDOS) defined as $\text{LDOS} = \sum_{j,\alpha} |\langle i\alpha | \psi_j \rangle|^2$ (where j runs over all eigenstates corresponding to single-particle energy-eigenvalues $|\epsilon_j| < 0.05W$ near the Fermi energy where W is the bandwidth of single-particle spectrum) at i -th unit cell with coordinate (x, y) and orbitals $\alpha = A, B$ at various times t . Unsurprisingly the edge-state evolution in topological situation ($0 < |\kappa| < 2$) follows the signatures of growth and shrinkage of clusters. We find that edge-modes are indeed localized at the boundary of clusters. When $n > n_c^{\text{Q}}$, the boundary of cluster grows in size with time t , while it shrinks and eventually vanishes when $n < n_c^{\text{Q}}$ (see Fig. 4(a,b)). However, when $\kappa = 0$ and $|\kappa| > 2$, given the trivial character of the nucleating droplets no such edge-modes can be localized on them. The evolution of such edge-state interface would be an interesting future study.

Outlook: In this work, we investigate nucleation processes of a scalar field when coupled to a topological fermionic field. Taking a concrete example of an Ising model coupled to a Chern insulator, we find that fermionic quantum fluctuations play an important role and lead to an additional contribution to surface tension of a nucleating cluster. Interestingly, the coupling parameter of the two fields can serve as a new tunable parameter for controlling the critical cluster-size in nucleation, thus affecting its growth and shrinkage. Ranging from implications on fundamental aspects of coupled topological field theories, just nucleation physics may also play a role in topological domains such as Chern mosaic structures seen in strongly correlated topological systems [56]. While our work involves coupling a two-dimensional Chern insulator, it opens up a range of

questions regarding physics of nucleation when coupled to higher dimensional topological systems, topologically ordered phases where fractionalization and entanglement can play distinctive roles.

Acknowledgements: We acknowledge fruitful discussions with Diptarka Das, Sabyasachi Chakraborty, Soumya Sur, Subrata Pachhal, Rahul Singh. S.M. acknowledges support from PMRF Fellowship, India. AA acknowledges support from IITK Initiation Grant (IITK/PHY/2022010). Numerical calculations were performed on the workstations *Wigner* and *Syahi* at IITK.

* msaikat@iitk.ac.in

† adhip@iitk.ac.in

- [1] K. Binder, Theory of first-order phase transitions, *Reports on Progress in Physics* **50**, 783 (1987).
- [2] P. M. Chaikin and T. C. Lubensky, *Principles of Condensed Matter Physics* (Cambridge University Press, 1995).
- [3] R. Livi and P. Politi, *Nonequilibrium Statistical Physics: A Modern Perspective* (Cambridge University Press, 2017).
- [4] V. M. Fokin, E. D. Zanotto, N. S. Yuritsyn, and J. W. Schmelzer, Homogeneous crystal nucleation in silicate glasses: A 40 years perspective, *Journal of Non-Crystalline Solids* **352**, 2681 (2006).
- [5] K. F. Kelton and A. L. Greer, *Nucleation in condensed matter*, Pergamon Materials Series (Pergamon, 2010).
- [6] H. Katsuno, K. Katsuno, and M. Sato, Effect of immobile impurities on two-dimensional nucleation, *Phys. Rev. E* **84**, 021605 (2011).
- [7] K. C. Chung, Nuclear fragmentation by nucleation approach, *Journal of Physics G: Nuclear and Particle Physics* **19**, 1373 (1993).
- [8] A. Strumia and N. Tetradis, A consistent calculation of bubble-nucleation rates, *Nuclear Physics B* **542**, 719 (1999).
- [9] A. Strumia and N. Tetradis, Testing nucleation theory in two dimensions, *Nuclear Physics B* **560**, 482 (1999).
- [10] B. Ali, I. J. Arnquist, D. Baxter, E. Behnke, M. Bressler, B. Broerman, K. Clark, J. I. Collar, P. S. Cooper, C. Cripe, M. Crisler, C. E. Dahl, M. Das, D. Durnford, S. Fallows, J. Farine, R. Filgas, A. García-Viltres, F. Girard, G. Giroux, O. Harris, E. W. Hoppe, C. M. Jackson, M. Jin, C. B. Krauss, V. Kumar, M. Lafreniere, M. Laurin, I. Lawson, A. Leblanc, H. Leng, I. Levine, C. Licciardi, S. Linden, P. Mitra, V. Monette, C. Moore, R. Neilson, A. J. Noble, H. Nozard, S. Pal, M.-C. Piro, A. Plante, S. Priya, C. Rethmeier, A. E. Robinson, J. Savoie, O. Scallon, A. Sonnenschein, N. Starinski, I. Štekl, D. Tiwari, F. Tardif, E. Vázquez-Jáuregui, U. Wichoski, V. Zacek, and J. Zhang (PICO Collaboration), Determining the bubble nucleation efficiency of low-energy nuclear recoils in superheated c_3f_8 dark matter detectors, *Phys. Rev. D* **106**, 122003 (2022).
- [11] M. B. Hindmarsh and T. W. B. Kibble, Cosmic strings, *Reports on Progress in Physics* **58**, 477 (1995).
- [12] F. R. Ares, O. Henriksson, M. Hindmarsh, C. Hoyos, and N. Jokela, Effective actions and bubble nucleation from holography, *Phys. Rev. D* **105**, 066020 (2022).
- [13] L. Giombi and M. Hindmarsh, General relativistic bubble growth in cosmological phase transitions, *Journal of Cosmology and Astroparticle Physics* **2024** (03), 059.
- [14] M. B. Enghoff, J. O. P. Pedersen, U. I. Uggerhøj, S. M. Paling, and H. Svensmark, Aerosol nucleation induced by a high energy particle beam, *Geophysical Research Letters* **38** (2011).
- [15] M. Eto and M. Nitta, Quantum nucleation of topological solitons, *Journal of High Energy Physics* **2022**, 77 (2022).
- [16] A. Ekstedt, Bubble nucleation to all orders, *Journal of High Energy Physics* **2022**, 115 (2022).
- [17] A. Tranberg and G. Ungersbäck, Bubble nucleation and quantum initial conditions in classical statistical simulations, *Journal of High Energy Physics* **2022**, 206 (2022).
- [18] J. Löfgren, M. J. Ramsey-Musolf, P. Schicho, and T. V. I. Tenkanen, Nucleation at finite temperature: A gauge-invariant perturbative framework, *Phys. Rev. Lett.* **130**, 251801 (2023).
- [19] J. Hirvonen, Nucleation rate in a high-temperature quantum field theory with hard particles (2024), arXiv:2403.07987 [hep-ph].
- [20] S. P. Kashyap, S. Mondal, A. Sen, and M. Verma, Surviving in a metastable de sitter space-time, *Journal of High Energy Physics* **2015**, 139 (2015).
- [21] R. Becker and W. Döring, Kinetische behandlung der keimbildung in übersättigten dämpfen, *Annalen der Physik* **416**, 719 (1935).
- [22] J. D. Gunton and M. Droz, *Introduction to the Theory of Metastable and Unstable States* (Springer, 1983).
- [23] P. G. Debenedetti, *Metastable liquids: concepts and principles* (Princeton university press, 2020).
- [24] P. A. Rikvold, H. Tomita, S. Miyashita, and S. W. Sides, Metastable lifetimes in a kinetic ising model: Dependence on field and system size, *Phys. Rev. E* **49**, 5080 (1994).
- [25] M. Acharyya and D. Stauffer, Nucleation and hysteresis in ising model: classical theory versus computer simulation, *The European Physical Journal B - Condensed Matter and Complex Systems* **5**, 571–575 (1998).
- [26] K. Brendel, G. T. Barkema, and H. van Beijeren, Nucleation times in the two-dimensional ising model, *Phys. Rev. E* **71**, 031601 (2005).
- [27] V. A. Shneidman and G. M. Nita, Collapse of transient nucleation fluxes in a cold ising ferromagnet, *Phys. Rev. Lett.* **97**, 065703 (2006).
- [28] S. Ryu and W. Cai, Validity of classical nucleation theory for ising models, *Phys. Rev. E* **81**, 030601 (2010).
- [29] S. van Teeffelen, C. N. Likos, and H. Löwen, Colloidal crystal growth at externally imposed nucleation clusters, *Phys. Rev. Lett.* **100**, 108302 (2008).
- [30] J. R. Savage and A. D. Dinsmore, Experimental evidence for two-step nucleation in colloidal crystallization, *Phys. Rev. Lett.* **102**, 198302 (2009).
- [31] D. M. Herlach, T. Palberg, I. Klassen, S. Klein, and R. Kobold, Overview: Experimental studies of crystal nucleation: Metals and colloids, *The Journal of Chemical Physics* **145**, 211703 (2016).
- [32] M. Dudek, E. A. Vik, S. V. Aanesen, and G. Øye, Colloid chemistry and experimental techniques for understanding fundamental behaviour of produced water in oil and gas production, *Advances in Colloid and Interface Science* **276**, 102105 (2020).
- [33] O. Fialko, M.-C. Delattre, J. Brand, and A. R. Kolovsky, Nucleation in finite topological systems during continu-

- ous metastable quantum phase transitions, *Phys. Rev. Lett.* **108**, 250402 (2012).
- [34] M. Z. Hasan and C. L. Kane, Colloquium: Topological insulators, *Rev. Mod. Phys.* **82**, 3045 (2010).
- [35] X.-L. Qi and S.-C. Zhang, Topological insulators and superconductors, *Rev. Mod. Phys.* **83**, 1057 (2011).
- [36] C.-K. Chiu, J. C. Y. Teo, A. P. Schnyder, and S. Ryu, Classification of topological quantum matter with symmetries, *Rev. Mod. Phys.* **88**, 035005 (2016).
- [37] Topological materials database, <https://topologicalquantumchemistry.com>.
- [38] B. Bradlyn, L. Elcoro, J. Cano, M. G. Vergniory, Z. Wang, C. Felser, M. I. Aroyo, and B. A. Bernevig, Topological quantum chemistry, *Nature* **547**, 298–305 (2017).
- [39] H. Wang, C. Du, P. Chris Hammel, and F. Yang, Spin current and inverse spin Hall effect in ferromagnetic metals probed by Y3Fe5O12-based spin pumping, *Applied Physics Letters* **104**, 202405 (2014).
- [40] J. Sinova, S. O. Valenzuela, J. Wunderlich, C. H. Back, and T. Jungwirth, Spin hall effects, *Rev. Mod. Phys.* **87**, 1213 (2015).
- [41] L. Šmejkal, J. Železný, J. Sinova, and T. Jungwirth, Electric control of dirac quasiparticles by spin-orbit torque in an antiferromagnet, *Phys. Rev. Lett.* **118**, 106402 (2017).
- [42] L. Šmejkal, Y. Mokrousov, B. Yan, and A. H. MacDonald, Topological antiferromagnetic spintronics, *Nature Physics* **14**, 242 (2018).
- [43] V. Bonbien, F. Zhuo, A. Salimath, O. Ly, A. About, and A. Manchon, Topological aspects of antiferromagnets, *Journal of Physics D: Applied Physics* **55**, 103002 (2021).
- [44] Y. Xue, W. Xu, B. Zhao, J. Zhang, and Z. Yang, Antiferromagnetic quantum spin hall insulators with high spin chern numbers, *Phys. Rev. B* **108**, 075138 (2023).
- [45] Z. Zhu, R. Liu, Y. Zhang, Y. Liu, Z. Yuan, and J.-W. Cai, Crossover from positive to negative spin hall signal in a ferromagnetic metal induced by the magnetization modulated interface effect, *Advanced Physics Research* **2**, 2300017 (2023).
- [46] A. Go, W. Witczak-Krempa, G. S. Jeon, K. Park, and Y. B. Kim, Correlation effects on 3d topological phases: From bulk to boundary, *Phys. Rev. Lett.* **109**, 066401 (2012).
- [47] B.-J. Yang and N. Nagaosa, Emergent topological phenomena in thin films of pyrochlore iridates, *Phys. Rev. Lett.* **112**, 246402 (2014).
- [48] W. Witczak-Krempa, G. Chen, Y. B. Kim, and L. Balents, Correlated quantum phenomena in the strong spin-orbit regime, *Annual Review of Condensed Matter Physics* **5**, 57 (2014).
- [49] A. Amaricci, A. Valli, G. Sangiovanni, B. Trauzettel, and M. Capone, Coexistence of metallic edge states and antiferromagnetic ordering in correlated topological insulators, *Phys. Rev. B* **98**, 045133 (2018).
- [50] L. Onsager, Crystal statistics. i. a two-dimensional model with an order-disorder transition, *Phys. Rev.* **65**, 117 (1944).
- [51] B. A. Bernevig, T. L. Hughes, and S.-C. Zhang, Quantum spin hall effect and topological phase transition in hgte quantum wells, *Science* **314**, 1757 (2006).
- [52] B. A. Bernevig, *Topological Insulators and Topological Superconductors* (Princeton University Press, Princeton, 2013).
- [53] L. O. J. K. Asbóth and A. Pályi, *A Short Course on Topological Insulators* (Springer Nature, 2016).
- [54] See supplemental material for analytical calculation of edge-mode energy per unit length and additional details on Monte Carlo simulation.
- [55] N. Metropolis, A. W. Rosenbluth, M. N. Rosenbluth, A. H. Teller, and E. Teller, Equation of State Calculations by Fast Computing Machines, *The Journal of Chemical Physics* **21**, 1087 (1953).
- [56] S. Grover, M. Bocarsly, A. Uri, P. Stepanov, G. D. Battista, I. Roy, J. Xiao, A. Y. Meltzer, Y. Myasoedov, K. Pareek, K. Watanabe, T. Taniguchi, B. Yan, A. Stern, E. Berg, D. K. Efetov, and E. Zeldov, Chern mosaic and berry-curvature magnetism in magic-angle graphene, *Nature Physics* **18**, 885–892 (2022).

Supplemental Material to “Surface Tension of a Topological Phase”

QUANTUM CORRECTION TO SURFACE TENSION IN TRIVIAL PHASE

In trivial phase ($|\kappa| > 2$), the quantum correction $\Delta\sigma$ to surface tension is much smaller compared to topological phase ($0 < |\kappa| < 2$). When $|\kappa| > 2$, $\Delta\sigma$ decreases with $|\kappa|$ (see Fig. S1(a)). Further, we find that when $|\kappa| > 2$, $\ln(\Delta\sigma)$ falls linearly with $\ln(|\kappa|)$, where slope < 0 (see Fig. S1(b)). This confirms that $\Delta\sigma$ in trivial phase decreases as a power-law with $|\kappa|$.

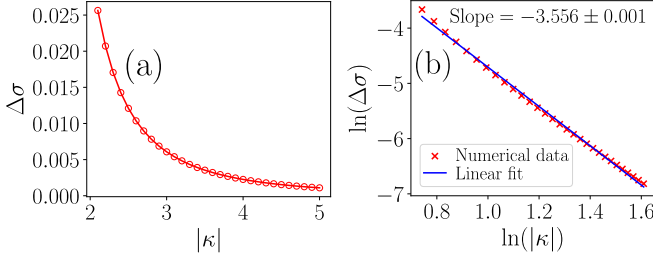


FIG. S1. **Quantum correction to surface tension in trivial phase:** (a) Quantum correction to surface tension $\Delta\sigma$ as a function of $|\kappa|$ for trivial phase ($|\kappa| > 2$), (b) $\ln(\Delta\sigma)$ as a function of $\ln(|\kappa|)$ and its linear fit for $|\kappa| \in [2.1, 5.0]$. For linear fit, slope < 0 , implying that $\Delta\sigma$ decreases as a power-law with $|\kappa|$ when $|\kappa| > 2$.

EDGE-MODE ENERGY PER UNIT LENGTH

To compute edge-mode energy per unit length for BHZ model, we consider the Hamiltonian

$$H = -M \sum_i \Psi_i^\dagger \sigma_z \Psi_i - \sum_{\langle ij \rangle} (\Psi_i^\dagger \eta_{ij} \Psi_j + \text{h.c.}). \quad (\text{S1})$$

For periodic boundary conditions in both x and y directions, we resort to momentum space where Hamiltonian for $k_x, k_y \in [-\pi, \pi]$ is

$$H_{k_x, k_y} = \sin(k_x)\tau_x + \sin(k_y)\tau_y + (-M - \cos(k_x) - \cos(k_y))\tau_z, \quad (\text{S2})$$

where τ_x, τ_y, τ_z are Pauli matrices. Thus, the dispersion relation is given by

$$\begin{aligned} E(k_x, k_y) &= \sqrt{\sin^2(k_x) + \sin^2(k_y) + (-M - \cos(k_x) - \cos(k_y))^2}. \end{aligned} \quad (\text{S3})$$

Now, in a ribbon geometry with periodic (open) boundary condition in x (y) direction, k_x remains a good quantum number and hosts x dispersing edge states on the

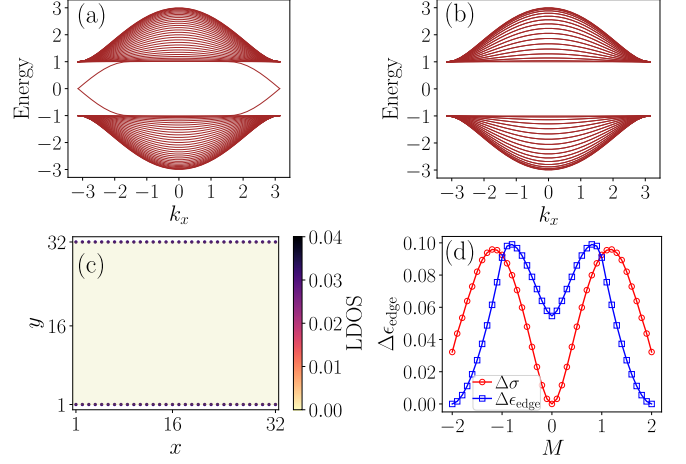


FIG. S2. **Edge-mode energy per unit length:** (a) Single-particle energy spectrum as a function of k_x for BHZ model with $M = 1.0$ for periodic boundary in x direction and open boundary in y direction, (b) single-particle energy spectrum as a function of k_x for BHZ model with $M = 1.0$ for periodic boundary in both x and y directions, (c) Local density of states (LDOS) of edge-modes at unit cell with coordinate (x, y) for BHZ model with periodic boundary in x direction and open boundary in y direction for $L = 32, M = 1.0$, (d) Quantum correction to surface tension ($\Delta\sigma$) and analytically calculated edge-mode energy per unit length $\Delta\epsilon_{\text{edge}}$ (see Eq. (S5)) as a function of $M \equiv \kappa$.

top and bottom boundaries. The dispersion in the two situations (open and periodic boundary conditions) and the local density of states (LDOS) of the edge-states are shown in Fig. S2(a-c).

The difference of the ground state energy for a half-filled system between the two situations (a) and (b) determines the mean edge-mode energy. An edge state wavefunction decaying exponentially in the y direction has an effective energy $E_{\text{edge}}(k_x) \sim |\sin(k_x)|$. However such an edge state can only be defined appropriately until it mixes with the bulk modes. The range of k_x until which the edge states survive is given by $\cos(k_x) = (-M + 1)$ when $0 < M < 2$ and $\cos(k_x) = (-M - 1)$ when $-2 < M < 0$. The valence bulk band energy $|E_{\text{valence}}(k_x)|$ is determined by $k_y = \pi$ mode when $0 < M < 2$ and $k_y = 0$ mode when $-2 < M < 0$. The difference thus is

$$\begin{aligned} \Delta E_{\text{edge}} &= \sum_{k_x} (|E_{\text{valence}}(k_x)| - E_{\text{edge}}(k_x)) \\ &= \frac{L}{2\pi} \int_{-\pi}^{\pi} dk_x (|E_{\text{valence}}(k_x)| - E_{\text{edge}}(k_x)). \end{aligned} \quad (\text{S4})$$

For a $L \times L$ square lattice with periodic boundary con-

dition in x direction and open boundary condition in y direction, the length of edge-modes is $2L$ when $|M| < 2$, as evident from the study of LDOS of edge-modes (see Fig. S2(c)). Therefore, edge-mode energy per unit length for $|M| < 2$ is

$$\Delta\epsilon_{\text{edge}} = \frac{\Delta E_{\text{edge}}}{2L} = \frac{1}{4\pi} \int_{-\pi}^{\pi} dk_x (|E_{\text{valence}}(k_x)| - E_{\text{edge}}(k_x)). \quad (\text{S5})$$

Comparison of $\Delta\epsilon_{\text{edge}}$ with the quantum correction to surface tension $\Delta\sigma$ (see main text) as a function of $M \equiv \kappa$ is provided in Fig. S2(d), where we find that $\Delta\sigma$ and $\Delta\epsilon_{\text{edge}}$ have same order of magnitude unless $\kappa \rightarrow 0$.

DETAILS OF MONTE CARLO SIMULATION

In Monte Carlo (MC) Simulation for classical Ising model ($\kappa = 0$), a random spin s_i is chosen and the energy ΔE_i required to flip the spin (i.e., $s_i \rightarrow -s_i$) is calculated. Thus,

$$\Delta E_i = 2Js_i \sum_{j \in \mathcal{N}} s_j + 2hs_i, \quad (\text{S6})$$

where j runs over all the nearest neighbours (\mathcal{N}) of i -th spin. Now, if $\Delta E_i < 0$ or if $p_i \leq \exp(-\beta\Delta E_i)$ for a randomly chosen $p_i \in [0, 1]$ where $\beta = 1/T$, the spin-flip is accepted and i -th spin becomes $-s_i$. If none of these two conditions is satisfied, the spin-flip is rejected and i -th spin remains s_i . Proceeding in this way, we compute $\langle s_{x,y} \rangle$ for all the spins at location (x, y) in Fig. 3(b,c,d) at time t in units of Monte Carlo steps per site (i.e. after tL^2 Monte Carlo steps where L^2 is number of spins in square lattice), where averaging is performed over a large number of MC simulations.

When classical Ising field is coupled to fermionic field ($\kappa \neq 0$), the quantum correction to surface tension $\Delta\sigma$ leads to the following modification in ΔE_i for the i -th spin:

$$\Delta E_i = 2Js_i \sum_{j \in \mathcal{N}} s_j + 2hs_i + (\Delta\sigma)s_i \sum_{j \in \mathcal{N}} s_j. \quad (\text{S7})$$

Thus, for $\kappa \neq 0$, acceptance or rejection of spin-flip is checked considering ΔE_i of Eq. (S7) in a similar way as done for $\kappa = 0$.